

Chromatin Accessibility and its Relationship to Pluripotency and the Induction of  
Pluripotent Stem Cells

A Thesis

SUBMITTED TO THE FACULTY OF THE UNIVERSITY OF MINNESOTA BY

Eric Espland

IN PARTIAL FULFILLMENT OF THE REQUIREMENTS  
FOR THE DEGREE OF  
MASTER OF SCIENCE

Adviser: Nobuaki Kikyo, MD, PhD

January 2015

Copyright © 2014

Eric Espland

All Rights Reserved

## Abstract

Chromatin within stem cells is dynamic and relaxed, allowing transcription and thus lineage specification to occur rapidly. To determine how this property can be used to enhance the generation of induced pluripotent stem cells (iPSC), I examined whether the expression of histone variants or peptidyl-prolyl isomerases (Ppiases) could increase the hyperdynamic, plastic nature of stem cell chromatin and thereby increase the efficiency and speed of reprogramming. I used molecular cloning to generate expression vectors containing the histone variants H3T and H2A.B. I used line-scanning microscopy to measure chromatin dynamics, with initial results suggesting that stem cells are more hyperdynamic in nature than differentiated cells. Although the research on the effect of histone variants and Ppiases on chromatin dynamics and reprogramming was not completed, another study showed that the expression of other histone variants does enhance reprogramming and may also induce an open chromatin structure. If this holds true for the histone variants studied here or Ppiase B (PpiB), this could further enhance the generation of iPSC and make future autologous engraftments of iPSC more feasible.

## Table of Contents

|                               |     |
|-------------------------------|-----|
| Table of Contents.....        | i   |
| List of Tables.....           | ii  |
| List of Figures.....          | iii |
| <br>                          |     |
| Chapter 1 – Introduction..... | 1   |
| Chapter 2 – Methods.....      | 15  |
| Chapter 3 – Results.....      | 23  |
| Chapter 4 – Discussion.....   | 36  |
| Chapter 5 – Bibliography..... | 39  |

## List of Tables

|   |    |
|---|----|
| Table 1 – Settings used during a standard PCR.....      | 15 |
| Table 2 – List of primers used and their sequences..... | 15 |

## List of Figures

|  |    |
|--|----|
| Figure 1 – Cloning of H3T into the pMXs-IP vector.....             | 24 |
| Figure 2 – Amplification of H2A.B and gH4.....                     | 26 |
| Figure 3 – PCR of HP1 $\alpha$ , HP1 $\beta$ , Ezh2 and Suz12..... | 29 |
| Figure 4 – Transfection of HP1 $\beta$ into MEFs.....              | 30 |
| Figure 5 – Vibratory motion of chromatin in ESC.....               | 31 |

## **1: Introduction**

### **1.1: Induced pluripotent stem cells: Past, present and future**

The history of induced pluripotent stem cells (iPSC) began in 1952 [5], when the first piece of evidence suggesting that differentiated cells retain the ability to become pluripotent emerged. Researchers were able to isolate nuclei from differentiated cells of an embryo in the blastocyst stage and transfer the nuclei into an anuclear oocyte [3]. The nucleated oocyte was then able to develop into a complete organism. This technique was the first recorded instance of reprogramming a differentiated cell to a pluripotent state and became known as somatic cell nuclear transfer (SCNT). In 1962, this was taken a step further, when a researcher discovered that he could use transfer nuclei from intestinal and skin cells from a completely mature frog to an oocyte and generate an entire organism [4]. These findings suggested two key ideas: that genetic information within the nuclei retain the ability to recapitulate any cell type of the body and that the cytoplasm of oocytes provided an environmental niche that supported reprogramming. In 2001, researchers found that fusion of mature differentiated cells with embryonic stem cells (ESC) caused the formation of pluripotent hybrids [6], [5], which suggested that the same factors found in environmental niche provided by oocytes are also found in ESC.

This led to breakthrough discovery in 2006, when researchers in Japan were able to reprogram mouse somatic cells into pluripotent cells by exogenous introduction of specific factors enriched in ESC [1]. By using a retrovirus to introduce the four transcription factors Oct3/4, Sox2, Klf4 and c-Myc (OSKM) into either mouse embryonic fibroblasts (MEF) or mature mouse fibroblasts, the researchers were able to generate cells

which were pluripotent (i.e. had the ability to generate any of the three germ layers) and had the ability to indefinitely self-renew. Just one year later, this same technique was found to be possible in humans using the transcription factors OCT4, SOX2, NANOG, and LIN28 [7].

Since its discovery, this iPSC generation technique (known as nuclear reprogramming) has been extensively refined. The use of viruses which directly integrate into the host genome (e.g. lentiviruses, retroviruses) carries the risk of interfering with endogenous gene function, which can lead to several diseases, including cancer [10]. Methods to deliver the transcription factors such as the use of non-integrating plasmid vectors [8], direct insertion of proteins [11], and the use of microRNAs [12] have been developed which do not carry these risks. Furthermore, the use of small-molecule chemical compounds to induce lineage specification in lieu of exogenous transcription factor expression has been developed [9]. Despite recent progress, however, the use of iPSC still has several shortcomings. The use of integrating vectors is prohibited in clinical settings due to its tumorigenicity [10]. Non-integrating vectors face a variety of different issues including low efficiency and slower reprogramming when compared to viral methods [10, 13]. Higher efficiency methods, such as the use of exogenous RNAs, have their own issues including the need for repeated transfections, the difficulty of synthesizing large RNA molecules, and the need for immunosuppression [10]. Direct additions of proteins have not yet been demonstrated as a valid method in human cells [10]. Furthermore, even without genomic integration, alternative mechanisms of mutagenesis can occur [10, 13]. Finally, the use of Oct4 expression levels as a readout of



reprogramming efficiency is dubious, due to the fact that not all cells expressing Oct4 become pluripotent [2]. This could lead to an overestimation of previously reported reprogramming efficiencies, typically between 0.001% and 5% [27]. Given this, it is evident that the discovery of additional factors and mechanisms through which efficient and safe reprogramming can occur will be greatly beneficial.

Importantly, the fact that when we change epigenetic factors such histone modifications (see section 1.2.2), we can enhance reprogramming efficiency [35] means that these epigenetic factors are a potential rate-limiting step in the reprogramming process and are therefore, a viable target for enhancing iPSC generation. Thus, the focus of this thesis is on how epigenetic factors can affect reprogramming and chromatin dynamics.

## **1.2: Chromatin and pluripotency**

### **1.2.1: Pluripotent stem cells transcribe more total genes than differentiated cells**

Although the exact mechanisms through which reprogramming occurs are not completely known, it is believed that a genome-wide loosening of chromatin plays a role [14]. In normal cell development, it has been demonstrated that genomes undergo a shift from a pluripotent state that is transcriptionally active to a mature differentiated state which is less transcriptionally active. For example, by visualizing expanding regions of heterochromatin (chromatin which is associated with transcriptional inactivity), it has been shown that a genome-wide closing of chromatin occurs during the differentiation of hematopoietic stem cells [14]. Furthermore, through qRT-PCR and microarray data it has

been shown that ESC are generally more transcriptionally active than differentiated cells [14, 18]. Quantitatively, ESC express up to 60% of all possible mRNAs, compared to just 10-20% in differentiated cells [14]. Most of these mRNAs are expressed at low yet detectable levels. Most interestingly, these mRNAs include genes which are not ESC-specific and are non-functional. Another study found that out of 600 protein-coding genes required for differentiation, a vast majority are upregulated in undifferentiated stem cells with only 69 being upregulated upon differentiation [29]. These studies point to a state of “leaky” transcription within undifferentiated stem cells.

### **1.2.2: Methods for measuring level of chromatin relaxation**

Current tools to test the level of accessibility of chromatin include studying histone modifications, chromatin remodeling complexes and chromatin architectural proteins. Histone modifications such as methylation and acetylation are events that alter the accessibility of DNA. One study found that the level of trimethylation of histone 3 on the 27<sup>th</sup> lysine (denoted H3K27me3), a modification that facilitates increased accessibility of the genome, is found genome-wide in cells undergoing reprogramming [19]. At loci where H3K4 trimethylation occurred, a coordinated decrease in the level of H3K27 trimethylation (an inactive gene marker) was found. Further studies have shown that this phenomenon is found with other epigenetic modifications as well. Active chromatin markers (e.g. H3K9 acetylation and H3K14 acetylation) are found in high levels in ESC while inactive markers (e.g. H3K9me3) are low in abundance [18]. However, in a phenomenon known as bivalent gene regulation, several promoters within ESC which are

developmentally important are paradoxically abundant in both H3K4me3 (an active marker) and H3K27me3 (an inactive marker) [25].

Another mechanism that enables the study of genome-wide chromatin changes is through ATP-dependent chromatin remodeling complexes [14]. These chromatin remodeling complexes allow access to the DNA for the purposes of DNA replication, repair, transcription and chromosome segregation [14]. The chromatin remodeling complexes are able to weaken the interactions within nucleosomes and cause a corresponding increase in chromatin relaxation [14]. It has been shown that these chromatin remodeling complexes are necessary for the maintenance and proliferation of ESC [20]. Inhibition or activation of these complexes is a potential tool in reprogramming. A key study found that when nucleosome remodeling and deacetylation complex (NuRD) was knocked out, reprogramming efficiencies increased [28]. Moreover, when a specific subunit of this complex, Mbd3, was inhibited, reprogramming efficiencies climbed further [28]. Another study found that inhibition of Chd1, a histone remodeling complex, resulted in an increase in the amount of heterochromatin and the inability to retain pluripotency and self-renewal in ESC [30].

Although the study of histone modifications and histone remodeling complexes can give us an idea of how accessible chromatin is, microscopy methods are capable of directly measuring the degree of dynamicity in chromatin through the study of scaffolding and structural proteins. It is possible to visualize the binding dynamics of these proteins through the use of fluorescence recovery after photobleaching (FRAP), a method that bleaches all fluorescence from a small area of chromatin and then measures

the time it takes for fluorescence to return to the bleached area. In this way, it is possible to measure the mobility of chromatin architectural proteins and therefore, the level of chromatin accessibility. A key study using this technique found that binding of major architectural proteins such as heterochromatin protein 1 $\alpha$  (HP1 $\alpha$ , a protein which binds to heterochromatin and regulates its formation) was hyperdynamic in ESC when compared to differentiated cells [21]. In other words, the architectural proteins were only loosely associated with ESC DNA. Upon differentiation, this binding was found to be much more permanent and the bound architectural components became immobile. Furthermore, that same study found that ESC which lacked HirA (a histone chaperone that facilitates nucleosome formation) had loosely bound histones and had accelerated embryoid body (EB) formation [21]. This study also found that, when elutions of varying salt concentrations were carried out, ESC DNA and histones were less tightly associated with each other when compared to three types of differentiated cells.

### **1.2.3: Chromatin in pluripotent stem cells exists is poised for activation**

Interestingly, ESCs have a chromatin morphology that is different from differentiated cells in that clusters of heterochromatin are less abundant yet larger and less physically condensed than the heterochromatin clusters found in differentiated cells [18]. The fact that these areas of heterochromatin do not bind to DNA as tightly as normal heterochromatin raises the question of its function. It is possible that this type of chromatin allows for easy genome accessibility while still being reasonably effective at repressing transcription to some extent. In this way, the genes required for lineage

specification would be poised for activation yet still transcriptionally silent. The existence of both bivalent transcriptional markers on key developmental genes in ESC [25], as well as the relatively loosely bound ESC heterochromatin [18, 21] and the fact that ESC have leaky transcription [14], all lend credibility to this theory.

### **1.3: Hypotheses**

In pluripotent stem cells, chromatin exists in a physically open yet mostly transcriptionally inactive state, with only leaky transcription occurring. The mechanism through which this occurs could be through a rapid vibration of the chromatin in which lineage specification regions are accessible but not necessarily actively transcribed in large quantities (a so-called “breathing” state). It is my hypothesis that this state can be proven through a novel microscopy method called line-scanning microscopy which allows the visualization of dynamic chromatin (see section 1.6.1). In addition, it is my hypothesis this state can be exploited by introducing factors which may facilitate the opening of chromatin in order to enhance reprogramming efficiency and speed. To test this, I first attempted to introduce histone variants that are associated with the opening of chromatin in differentiated cells. Second, I attempted to introduce factors from a class of proteins known as Ppiases, which also may facilitate the opening of chromatin. To test whether these two classes of factors have a role in the opening of chromatin, I planned to utilize the line-scanning microscopy method to measure chromatin dynamics as well as FRAP to measure the mobility of architectural proteins (and thus, the accessibility of chromatin). Finally, I planned to introduce these factors into differentiated cells along

with OSKM and determine if these factors are capable of improving reprogramming efficiency and speed.

#### **1.4: Histone variants**

Histones are an octamer of subunits (H2A, H2B, H3 and H4) and are linked together through the linker histone H1. These histones (known as canonical histones) are deposited into chromatin during replication via chaperone proteins, which escort the variants to the chromatin and facilitate their insertion [31]. However, several variants have been identified that differ from the canonical histones in terms of binding tightness (and the corresponding level of chromatin relaxation) and in terms of what stage of development they are expressed [23]. Some of these histone variants are deposited in a replication-independent manner. Because of this, certain histone variants can account for up to 90% of the histones in terminally differentiated cells which rarely divide [31]. The incorporation of these variants is not merely an incidental occurrence during normal development; it has been shown that these events are key mediators of chromatin remodeling and epigenetic changes, including transcriptional activation, transcriptional repression, and chromosomal segregation [23, 31]. For example, the histone variants macroH2A and H3.3 are highly upregulated in oocytes [23] while another histone variant (H3T) is specific to testis [25]. MacroH2A is associated with transcriptionally repressed genes and has been shown to be incorporated at a higher rate as ESC differentiate [31]. Other studies have shown that histone variants also have a role in pluripotency and self-renewal. For example, a study showed that when they took ESC and knocked out H2A.Z,

a variant that associates with the binding sites of pluripotency genes, they found that chromatin accessibility was decreased, which resulted in a decrease in the efficiency of self-renewal [31, 32].

Early SCNT experiments provide evidence that oocytes contain factors that are able to reprogram differentiated cells into iPSC. However, the fact that the OSKM factors are not highly expressed in oocytes [24] leads us to believe that there must be other factors present within the oocyte that can facilitate reprogramming. Taken together with the key role that histone variants play in spermatogenesis, oocyte function and early embryonic development, this means that it is possible that the exogenous expression of histone variants could facilitate reprogramming with OSKM by opening chromatin.

#### **1.4.1: Histone variant H3.3**

This led us to investigate which histone variants would be most appropriate for the purpose of reprogramming enhancement. Of these variants, the first one that we considered investigating was H3.3. The H3.3 from oocytes is used to replace protamine (a surrogate histone-like protein which confers an extremely tightly packed genome) upon fertilization [31]. Interestingly, H3.3 was found to be associated with the bivalent promoters of the ESC genes discussed in section 1.2.2 [33]. Because H3.3 is associated with both transcriptionally active and repressed genes, it is thought that H3.3 plays a role in the maintenance of this bivalent state [31]. Another study found that H3.3 deposition is necessary for reprogramming to occur in SCNT in *Xenopus* [36]. Although this seems like a promising avenue of research, this study was only performed in *Xenopus* through a

pathway which is not found in mammals [36]. In addition, due to the fact that crystal structure of human H3.3 has no defining structural features which would be firmly associated with either open and closed chromatin, we did not pursue H3.3 further.

#### **1.4.2: Histone variant H3T**

Another variant, H3T, had a very high similarity to canonical histones H3.1 and H3.2 (87-88% amino acid sequence conservation in GenBank sequences compared using Serial Cloner). It is 411bp in length and is expressed in the testes. Importantly, its structure was found to be inherently unstable [37]. Using FRAP, this same study also found that H3T deposited into chromatin at a faster rate than the canonical H3.1. Additionally, H3T might be part of the 4% of histones that are not replaced by protamine in spermatogenesis and that are enriched around developmentally important genes, such as the Hox genes [38]. Based on this, we hypothesized that overexpression of the testes specific variant H3T may enhance reprogramming via chromatin relaxation.

#### **1.4.3: Histone variant H2A.B**

Another variant that we decided to investigate was H2A.B, a variant highly expressed in testes and at low levels in the brain [31] and was found to be enriched at the transcriptional start site of many active genes [34]. Importantly, it was also found to play an important role in the activation of the paternal genome following fertilization by means of its incorporation into the inactive X-chromosome and activating a multitude of genes [34]. Structurally, this variant does not have a domain that is known to cause the



compaction (and thus the silencing) of chromatin [34]. In addition, H2A.B is known to associate and dissociate with chromatin in a rapid manner, facilitating its reorganization [39]. Based on these findings, we hypothesized that overexpression of H2A.B will lead to a higher level of hyperdynamic chromatin and therefore, easier activation of pluripotency genes in the ESC genome and a higher and faster reprogramming process.

### 1.5: Ppiases

A group of proteins known as peptide prolyl isomerases (Ppiases) have a variety of roles in eukaryotic cells. Their primary function is to catalyze the change in orientation (from *cis* to *trans* or vice versa) of peptide bonds [41]. This group of proteins plays a variety of roles, including protein folding and post-translational regulation of cellular components. For example, a Ppiase named Pin1 can induce a conformational change in c-Myc which leads to the ubiquitination and subsequent degradation of c-Myc [42]. Inhibition experiments of Pin1 have shown that it is essential for maintenance of pluripotency and self-renewal. Interestingly, another Ppiase named Fpr4 was found to be capable of regulating transcriptional status via the isomerization of histone H3 [43]. Another group of Ppiases (which is the focus of this thesis) are known as cyclophilins. Although cyclophilins have been characterized as having diverse physiological roles, including programmed cell death [44], they are all characterized by the same peptide prolyl isomerase activity. They have not yet been linked to pluripotency and self-renewal. It is possible that some of the members of the cyclophilin family (also known as simply Ppiases) could be able to isomerize prolyl residues within histones, as seen in Pin1.

Through this mechanism, it is possible that cyclophilins are able to relax chromatin and thereby enhance reprogramming.

To assess this possibility, I planned to clone the Ppiases, express them in bacteria, purify the protein, and then perform what is called a Ppiase assay [45]. This assay essentially takes a small sequence of amino acids (in our case, the amino acids found within the histone tails) which contains a prolyl residue and is incubated with chymotrypsin conjugated to *p*-nitroaniline [46]. If the purified protein does have *cis-trans* isomerase at that specific amino acid sequence, the *p*-nitroaniline will be cleaved and will fluoresce. If any of the purified proteins do have isomerase activity for any of the histone tails, we will then characterize their ability to relax chromatin using line-scanning microscopy and FRAP.

## **1.6 Methods for determining accessibility of chromatin**

### **1.6.1 Line-scanning microscopy and chromatin of pluripotent cells**

To test my hypothesis on the so called “breathing” chromatin, I used a form of imaging known as line-scanning microscopy [40]. Previous methods do not provide a high enough temporal or spatial resolution to capture the vibrational motion of chromatin, which happens on the order of microseconds and nanometers. Line-scanning microscopy involves staining the DNA using a non-specific Hoechst 33342 dye and zooming in on the chromatin. The machine then scans a line directly across the DNA and measures the fluorescence intensity at each pixel. This scan occurs fast enough to capture small, quick movements by chromatin. The line scan is then repeated thousands of times to generate

the location of the mean intensity as a function of time. Then, using a mathematical tool known as autocorrelation which allows us to determine how often the location of mean intensity is in the same place, we can determine how repetitive this motion is. For example, if the mean intensity of fluorescence repeatedly deviates from one point in space but returns back to that same point again and again, it would have a high autocorrelation constant. This high autocorrelation constant is therefore a readout of oscillatory motion. If we are able to determine whether chromatin oscillates rapidly in ESC compared to differentiated cells, this would provide evidence for a vibratory “breathing” chromatin state. One group has previously used this method to compare ESC to MEFs [40] and found that there is an oscillatory motion in ESC that is not found in MEF. However, this experiment has not been repeated and the method has not been used to study the effect of protein interactions on the motion of chromatin. Our goal was to use the method to confirm the previous group's finding and so that it could be used in other experiments, such as the effect of the incorporation of histone variants or the effect of architectural proteins on the motion of chromatin.

### **1.6.2: FRAP of heterochromatin binding proteins**

As described in section 1.2.2, the use of FRAP allows us to directly measure the degree of chromatin accessibility by monitoring the mobility of chromatin binding proteins. In humans, the polycomb repressive complex 2 (PRC2) mediates the silencing of genes through H3K27 trimethylation, which enables the binding of a different polycomb repressive complex, PRC1 [47]. This complex is made of the subunits Ezh2,

Suz12, Eed, and RbAP48. By studying the binding kinetics of these proteins to chromatin, we will be able to directly measure the accessibility of chromatin. In addition, previous studies have used heterochromatin proteins  $1\alpha$  and  $1\beta$  (HP1 $\alpha$  and HP1 $\beta$ ) to measure chromatin accessibility. In particular, I plan on cloning HP1 $\alpha$ , HP1 $\beta$ , Suz12 and Ezh2 attached to a GFP reporter in order to express these proteins in mammalian cells to visualize chromatin binding dynamics via FRAP. If binding is transient (i.e. the recovery time measured via FRAP is low), this is indicative of hyperdynamic open chromatin while longer lasting binding will be indicative of silenced chromatin.

In this thesis, I will first clone two classes of genes (histone variants and Ppiases) and express them in differentiated cells. Using FRAP and line-scanning microscopy, I will then determine if the expressed genes cause the chromatin to become hyperdynamic and more accessible. If it is true that these factors are able to effect change in chromatin dynamics, I will then assess their ability to improve reprogramming efficiency and speed.

## 2: Methods

### 2.1: Histone variant cloning

#### 2.1.1: H3T (pMXs-IP)

The H3T gene was amplified from the pEGFP-C3-H3T using primers H3T cF1 and H3T cR1. The primers contained a His-tag on the N-terminus. The primers (Life Technologies) were received in their solid state and were resuspended in water which had been UV treated. The PCR conditions were optimized using either Q5 polymerase or Pfx polymerase. The standard PCR conditions are listed in Table 1. The primer sequences used are listed in Table 2.

| Process: Temperature   | Time (s) |
|------------------------|----------|
| Denaturing: 94°C       | 15       |
| Annealing: 55°C        | 30       |
| Elongation: 68°C       | 60       |
| Final elongation: 68°C | 420      |
| Final hold: 4°C        | ∞        |

*Table 1: Settings used during a standard PCR. The first 3 steps were cycled 25 times*

| Primer name | Sequence   |
|-------------|--|
| H3T cF1     | CGAGAATTCATGGACTACAAAGACG<br>ATGACGACAAGGCTCGTACTAAACA<br>GACAGCTCGG |
| H3T cR1     | CGAGCGGCCGCCTACGCTCTTTCTCC<br>GCGAAT                                 |
| H2A.B cF2   | CGAGAATTCATGGACTACAAAGACG<br>ATGACGACAAGACGATGACGACAAG               |

|                  |  |
|------------------|--|
|                  | CCGAGGAGGAGGAGACGCC  |
| H2A.B cR2        | CGAGCGGCCGCCTAGTCCTCGCCAG<br>GGGCC                                   |
| gH4 cF1          | ATGCGGATCCATGGACTACAAAGAC<br>GATGACGACAAGTCTGGCAGAGGAA<br>AGGGTG     |
| gH4 cR1          | CTAGCTCGAGCTAGCCTCCGAAGCC<br>GTAG                                    |
| HP1 $\alpha$ cF3 | TTTTTTGGTACCATGGGAAAGAAGAC<br>CAAGAG                                 |
| HP1 $\alpha$ cR3 | TTTTTTGGATCCTTAATGATGATGATG<br>ATGATGGCTCTTCGCGCTTTCTT               |
| HP1 $\beta$ cF3  | TTTTTTGGTACCATGGGGAAAAAGCA<br>AAACAA                                 |
| HP1 $\beta$ cR3  | TTTTTTGGATCCCTAATGATGATGATG<br>ATGATGATTCTTGTCGTCTTTTTTGTC           |
| Ezh2 cF3         | TTTTTTAGATCTATGGGCCAGACTGG<br>GAAG                                   |
| Ezh2 cR3         | TTTTTTGGATCCTCAATGATGATGATG<br>ATGATGAGGATTCCATTTCTCGTTC<br>G        |
| Suz12 cF3        | TTTTTTGGTACCATGGCGCCTCAGAA<br>GCA                                    |
| Suz12 cR3        | TTTTTTGGATCCTCAATGATGATGATG<br>ATGATGGAGTTTTTGTTTCTTGCTCT<br>GTTTTGG |

|          |  |
|----------|--|
| PpiB cF1 | TTTTTTCATATGCTGCGCCTCTCGG                              |
| PpiB cR1 | TTTTTCTCGAGCTAATGATGATGATG<br>ATGATGCTCCTTGGCAATGGCGAA |
| PpiC cF1 | TTTTTTCATATGAGCCCGGGTCCC                               |
| PpiC cR1 | TTTTTCTCGAGTCAATGATGATGAT<br>GATGATGCCAATCAGGGACCTCAA  |
| PpiD cF1 | TTTTTTCATATGTCCACGCGATCC                               |
| PpiD cR1 | TTTTTCTCGAGTTAATGATGATGATG<br>ATGATGAGCAAACATTTTGCATAC |
| PpiH cF1 | TTTTTTCATATGGCGGTGGCAAAT                               |
| PpiH cR1 | TTTTTCTCGAGTTAATGATGATGATG<br>ATGATGCATTTCCCCACACTGT   |
| PpiA qF1 | AGGTCCATCTACGGAGAGAAA                                  |
| PpiA qR1 | AGTCTTGGCAGTGCAGATAAA                                  |
| PpiB qF1 | CAGGAGGAAAGAGCATCTATGG                                 |
| PpiB qR1 | GGAGGTCTTGACTGTGGTTATG                                 |
| PpiC qF1 | GGAGACAAAGATGTGGGTAGAA                                 |
| PpiC qR1 | CTTGATGACACGGTGGAAGA                                   |
| PpiD qF1 | ACGAATGGCTCTCAGTTCTTT                                  |
| PpiD qR1 | CTTGCCACACCTAGTCCTTT                                   |
| PpiE qF1 | TGTGTCAGGGTGGTGATTTC                                   |
| PpiE qR1 | GGTCCTGTGTGTTTAAGGATGA                                 |
| PpiF qF1 | CACCAATGGCTCTCAGTTCTT                                  |
| PpiF qR1 | CACAACATCCATGCCCTCTT                                   |
| PpiG qF1 | CTAAAGCCGATGACAAGGAGAG                                 |
| PpiG qR1 | CTAAGAATCGTCGCTGGTATGAA                                |
| PpiH qF1 | CAGTCAATCCAGTGGTCTTCTT                                 |
| PpiH qR1 | CCTAAAGTTCTCTGCCGTCTTAG                                |

Table 2: List of primers used and their sequences

The amplified gene fragment was then subjected to electrophoresis on a 0.8% agarose gel. The fragment was extracted and purified using the Promega Wizard SV Gel and PCR Clean-up Kit. The isolated gene was then digested using EcoRI and NotI. The digested gene product was then gel-purified using the Promega Wizard SV Gel and PCR Clean-up Kit.

The mammalian expression retroviral vector pMXs-IP was digested and column-purified using the Promega Wizard SV Gel and PCR Clean-up Kit. The digested gene was then ligated into the digested pMXs-IP vector using T4 Ligase, 10x T4 buffer and a 3:1 molar ratio of H3T:pMXs-IP. The ligation reaction was incubated at 23°C for 1 hour.

The ligation product was then transformed into competent DH5α *E. coli* cells. The competent cells were mixed with 5μl of the ligation reaction. The cells were then heat shocked at 42°C. 500μl of LB was added and the mixture was shaken at 200rpm and 37°C for 1 hour. The cells were then plated onto plates containing LB media with ampicillin and grown at 37°C overnight. The colonies were then inoculated in liquid LB with ampicillin and incubated overnight at 37°C. The plasmids from these liquid cultures were then purified using the Thermo Scientific GeneJET Plasmid Miniprep Kit. The plasmids were then digested with NotI and EcoRI to ensure that the gene product was inserted. The colonies which presumably had a complete copy of the gene were sequenced. 200ng of the pMXs-IP plasmid was mixed with 1μl of 6.4μM H3T sF1 sequencing primer. The mixture was sent to the University of Minnesota Genomics Center. The sequences were then analyzed and compared to the reported sequence using Serial Cloner software.



### **2.1.2: H2A.B (pMXs-IP)**

The H2A.B gene was amplified from the pcDNA3.1-CT-GFP-H2A.B plasmid which was obtained from Addgene [11]. H2A.B was cloned into the pMXs-IP plasmid. The plasmid was prepared as described in section 2.1.1.

H2A.B cF2 and H2A.B cR2 primers were used for PCR. EcoRI and NotI restriction enzymes were used. The gel-extraction, purification, ligation and transformation were performed as described in 2.1.1.

### **2.1.3: gH4**

Reverse transcriptase (Superscript III, Life Technologies) and the Total RNA Qiagen kit were used to produce cDNA from mouse embryonic stem cells (mESC). The germinal H4 gene was cloned using the mESC cDNA as a template. The PCR conditions and further experiments were performed as described in section 2.1.1.

gH4 cR1 and gH4 cF1 primers were used for PCR. BamHI and XhoI restriction enzymes were used. The gel-extraction, purification, ligation and transformation were performed as described in 2.1.1.

## **2.2: Cloning of heterochromatin genes**

### **2.2.1: HP1 $\alpha$ , HP1 $\beta$ , Ezh2 and Suz12**

The HP1 $\alpha$ , HP1 $\beta$ , Ezh2 and Suz12 genes were amplified from the p5G5 plasmid containing the genes. The HP1 $\alpha$ , HP1 $\beta$ , and Ezh2 genes were then cloned into both the pMX-GFP and pEGFP plasmids. The plasmids were prepared as described in section

### 2.1.1.

The primers used for the PCR of HP1 $\alpha$ , HP1 $\beta$ , Ezh2 and Suz12 were HP1 $\alpha$  cF3, HP1 $\alpha$  cR3; HP1 $\beta$  cF3, HP1 $\beta$  cR3; Ezh2 cF3, Ezh2 cR3; Suz12 cF3, Suz12 cR3 respectively.

The gel-extraction, purification, ligation and transformation were performed as described in 2.1.1.

## 2.3 Cloning of Ppiase genes

### 2.3.1: PpiB, PpiC, PpiD and PpiH

The PpiB, PpiC, PpiD and PpiH genes were amplified from mESC cDNA as prepared in section 2.1.3. The genes were cloned into the pEGFP-C1 plasmid. The plasmid was prepared as described in section 2.1.1.

The primers used for the PCR of PpiB, PpiC, PpiD and PpiH were PpiB cF1, PpiB cR1; PpiC cF1, PpiC cR1; PpiD cF1, PpiD cR1; PpiH cF1, PpiH cR1 respectively. The gel-extraction, purification, ligation and transformation were performed as described in 2.1.1.

## 2.4: CGR8 mESC culture

The mouse ESC line CGR8 was used. The cells were maintained in a 3.5cm dish. The cells were washed twice with 3ml of Phosphate Buffered Saline (PBS). 0.5ml of trypsin was added and incubated at 37°C for 5 minutes. 2ml of Dulbecco's Modified Eagle's Medium (DMEM) and 10% Fetal Bovine Serum (FBS) (Life Technologies ) was

added. The cells were then counted and were spun down at 1000rpm at 4°C for 5 minutes. The pellet was resuspended in Glasgow's Minimum Essential Medium (GMEM) (Life Technologies ) and Leukemia Inhibitory Factor (LIF) (EMD Millipore™) . The cells were seeded onto a 3cm dish for further passaging (1:5 ratio used). The media was changed every day and the cells were passaged every 2-3 days.

## **2.5: Transfection**

The CGR8 cells were transfected using Invitrogen Life Technologies Lipofectamine 2000 DNA Transfection Kit.

## **2.6: Immunofluorescence staining**

The CGR8 cells were washed twice with 1ml of PBS. 1ml of 4% Paraformaldehyde (PFA) in PBS was added and incubated at 23°C for 10 minutes. The cells were permeabilized using 1ml of 0.5% Triton X and incubated at 23°C for 10 minutes. The cells were then washed twice using 500µl of washing buffer containing PBS, FBS, Tween 20 and water. A 1:500 dilution of 0.5µg/µl primary antibody (6x-His Epitope Tag (Catalog # OAEA00010) from Aviva Systems Biology) was added and incubated at 23°C for 1 hour. The cells were then washed again using 500µl of the washing buffer. A 1:200 dilution of 1µg/µl secondary antibody (Alexa Fluor R555 from Invitrogen Life Technologies) was then added and incubated at 23°C for 1 hour in the dark. DNA was counterstained with 1µg/ml Hoechst 33342. The cells were then washed with PBS and observed.

## **2.7: Line-scanning Microscopy**

The CGR8 cells were washed twice with 1ml of PBS. The DNA was stained non-specifically using 1 $\mu$ g/ml Hoechst 33342 and incubated at 23°C for 10 minutes. The cells were then washed twice again with PBS and 2.5ml of fresh medium was added.

The cells were then brought to the University of Minnesota Imaging Center. Microscopes used included the Nikon A1 Spectral Confocal Microscope and the Olympus FluoView FV1000 IX2 Inverted Confocal Microscope. The Olympus microscope scanned up to 32,000 lines containing 32 pixels per line, with each pixel representing 82nm. The Nikon microscope scanned up to 200,000 lines with each pixel representing down to 8nm. The dwell time for each pixel varied between 0.5 and 2 $\mu$ sec/pixel. Higher pixel resolution, larger dwell times, more line scans also resulted in more accurate fluorescence readings but a higher rate of photobleaching. Both unidirectional and bidirectional line scans were used. A 405nm excitation laser was used.

## **2.8: qRT-PCR**

mESC cDNA prepared in section 2.1.3 was used as a template. 30 cycles were used. Primers used are listed in Table 2. Microsoft Excel was used to analyze the resultant data.

### **3: Results**

#### **3.1: Cloning of histone variants into expression vectors**

##### **3.1.1: Cloning of H3T into the pMXs-IP expression vector**

A PCR was run on the pEGFP-C3-H3T plasmid but no gene product was obtained. The PCR settings were revised with a higher annealing temperature (60°C). This was chosen due to the suggested annealing temperature from Applied Biosystems [9]. Again, no band was obtained. The primers were then redesigned to have a higher affinity for the DNA and a subsequent higher annealing temperature. The PCR was repeated and a faint 400bp band was produced. The PCR was repeated with more initial template DNA and an increased number of cycles in order to increase the concentration of the gene product. The PCR produced a bright 400bp band and a faint 800bp band. The 400bp band was then extracted and purified (Figure 1A). The gene was then successfully ligated to the pMXs-IP plasmid and transformed. 5 colonies were chosen for liquid cultures. All 5 liquid cultures showed a distinct 400bp band upon digestion of the extracted plasmid (Figure 1B). 3 of the plasmids were sequenced and all had a 100% match to the reported sequence. This project was halted due to a paper being published on the role of histone variants in reprogramming [24].

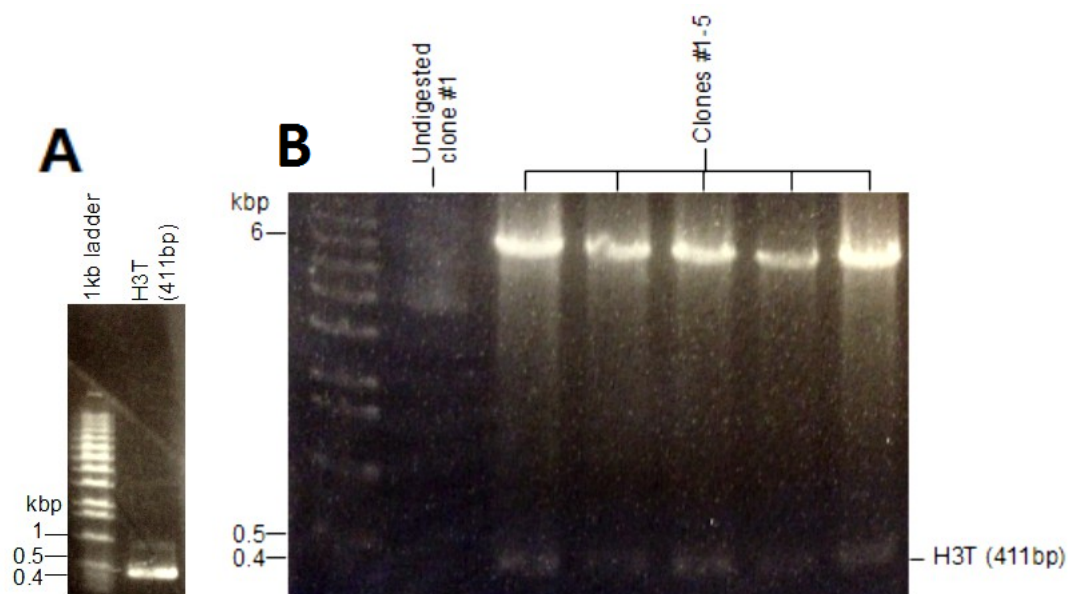


Figure 1: Cloning of H3T into the pMXs-IP vector (A) PCR of H3T gene (B) Diagnostic digest of pMXs-IP-H3T constructs. Completed constructs were digested with restriction enzymes that would cleave the gene out of the vector to ensure its proper insertion

### 3.1.2: Cloning of H2A.B into the pMXs-IP expression vector

A two-step PCR cycle was used. The initial PCR produced a band that was approximately 350bp in length. The PCR was repeated to increase total DNA. A distinct 350bp band was again obtained (Figure 2). The gene product was then digested and column-purified. The ligation reaction failed to transform successfully and produced no colonies. The ligation was repeated with an increase in the insert to vector ratio. The ligation failed again.

It was suspected that the competent cells were the root cause of the transformation failures. To test this, closed-circle pMXs-IP-H3T was transformed using the same transformation protocol. Over 200 colonies were obtained. It was concluded that the competent cells were not the cause of the previous failures.

It was then hypothesized that there was something wrong with either the PCR or the ligation process. To address this, the cloning of H2A.B was repeated with all new reagents, including fresh ligation buffer and newly autoclaved water. The total number of cycles in the PCR was set at 35. A different clone of the initial pcDNA3.1-CT-H2A.B was used as a template. A distinct band at 350bp was obtained. The ligation failed again. It was hypothesized that the NotI enzyme was not active, due to its expiration date. A new enzyme was obtained and used. The ligation failed again.

### **3.1.3: Cloning of gH4 into the pMXs-IP**

gH4 cDNA was successfully amplified from the mESC template DNA using 40 cycles in the PCR. A band approximately 300bp in length was obtained along with an additional faint band approximately 600bp in size. It was believed that this faint band was a result of an excessive number of cycles used. The PCR was repeated with only 35 cycles, resulting in a single distinct 300bp band was obtained, confirming our hypothesis about the number of cycles (Figure 2). After digestion and purification, the gene was ligated to its target plasmid. Just as was seen in the H2A.B cloning, the ligation was unsuccessful. The steps listed in section 3.1.2 were attempted. The ligation and transformation were ultimately unsuccessful.



Figure 2: Amplification of H2A.B and gH4 (second round of PCR shown)

### 3.2: Cloning of heterochromatin genes into expression vectors

#### 3.2.1: Mutagenesis of pMX-GFP

A mutagenic PCR reaction was carried out in order to introduce an XhoI and PacI site into the pMXs-GFP plasmid. DpnI was used to digest all methylated DNA which would not have undergone mutagenesis. Upon digestion of the mutated plasmid with XhoI and PacI independently, open circular DNA plasmids were obtained, indicating the mutagenesis was successful.

#### 3.2.2: Cloning of HP1 $\alpha$ into pEGFP-C1 and pMX-GFP

A gene product of approximately 550bp was successfully cloned from the p5G5-HP1 $\alpha$  plasmid, along with an additional band. The 550bp gene product was then



extracted and purified (Figure 3).

The gene product and the mutagenic pMXs-IP plasmid were then ligated and transformed. The ligation was unsuccessful for pMXs-IP-HP1 $\alpha$ . After many unsuccessful attempts at ligation (see section 3.1.2 for experiments tried), we shifted focus onto solely the pEGFP plasmid. The pEGFP ligations repeatedly produced closed circle plasmids with no insert. At this time, the ligation to the pEGFP-C1 plasmid was successfully performed by Hiroshi Kobayashi using a Calf Intestinal Alkaline Phosphatase (CIP) treatment. It was discovered that the two digestion enzymes being used (BglII and BamHI) had compatible sticky ends, causing the plasmid to preferentially undergo self-ligation. Dr. Kobayashi's construct was sequenced and found to be a 100% match to the reported sequence.

### **3.2.3: Cloning of HP1 $\beta$ into pEGFP-C1 and pMX-GFP**

A 550bp band along with an additional band were produced from the PCR. The 550bp band was gel-extracted and purified (Figure 3). The ligation to the pMX-GFP plasmid was repeatedly unsuccessful (see section 3.1.2). Unlike our experiments with HP1 $\alpha$ , the ligation to the pEGFP plasmid was successful without the need for Dr. Kobayashi's CIP treatment. The sequence of this construct was a 100% match to the reported sequence.

### **3.2.4: Cloning of Ezh2 into pEGFP-C1 and pMX-GFP**

A single band approximately 2200bp in size was produced from the PCR and

column-purified (Figure 3). The ligation to the pMX-GFP plasmid was again repeatedly unsuccessful (see section 3.1.2). The ligation to the pEGFP plasmid was successful. Due to the length of the insert, we decided to sequence only the first 500bp of the 5' end. The sequence of this section was a 100% match to the reported sequence.

### **3.2.5: Cloning of Suz12 into pEGFP-C1 and pMX-GFP**

During the initial PCR of Suz12, no gene products were obtained. Believing that there might not be enough template DNA, we increased the initial amount of DNA. Again, no bands were obtained. We then tried lowering the annealing temperature, resulting in multiple bands but none being the correct size (Figure 3). We then redesigned the primers to have a lower annealing temperature. However, no bands were obtained. Again, we tried lower annealing temperatures with the new primers and again, multiple bands of the incorrect size were produced. Suz12 was ultimately unable to be cloned from its plasmid due to trouble optimizing the PCR.

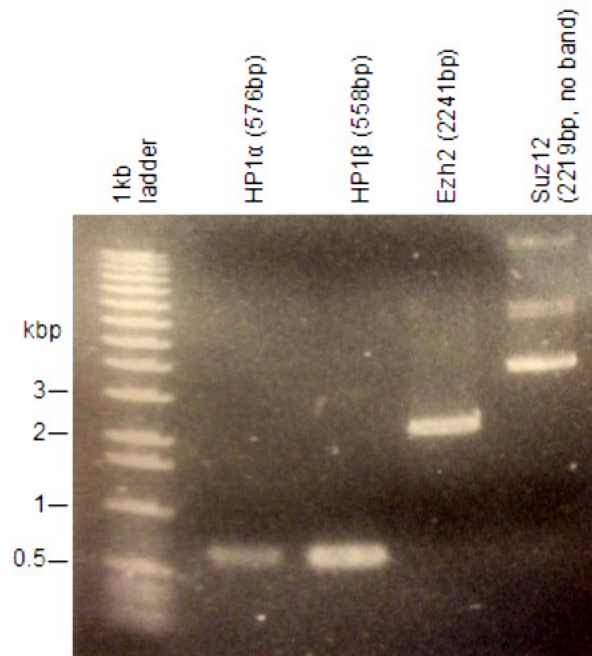


Figure 3: PCR of selected genes. HP1 $\alpha$ , HP1 $\beta$ , and Ezh2 amplification successfully produced bands of the correct size. Amplification of Suz12 was unsuccessful.

### 3.2.6: Transfection of HP1 $\alpha$ and HP1 $\beta$ into CGR8 cells

The pEGFP-HP1 $\alpha$  and pEGFP-HP1 $\beta$  constructs were then successfully transfected into CGR8 cells following the protocol in section 2.5. The pEGFP-Ezh2 was also attempted to be transfected, although it was unsuccessful. The transfection efficiency was about 5% for HP1 $\alpha$  and about 1-2% for HP1 $\beta$  (Figure 4A).

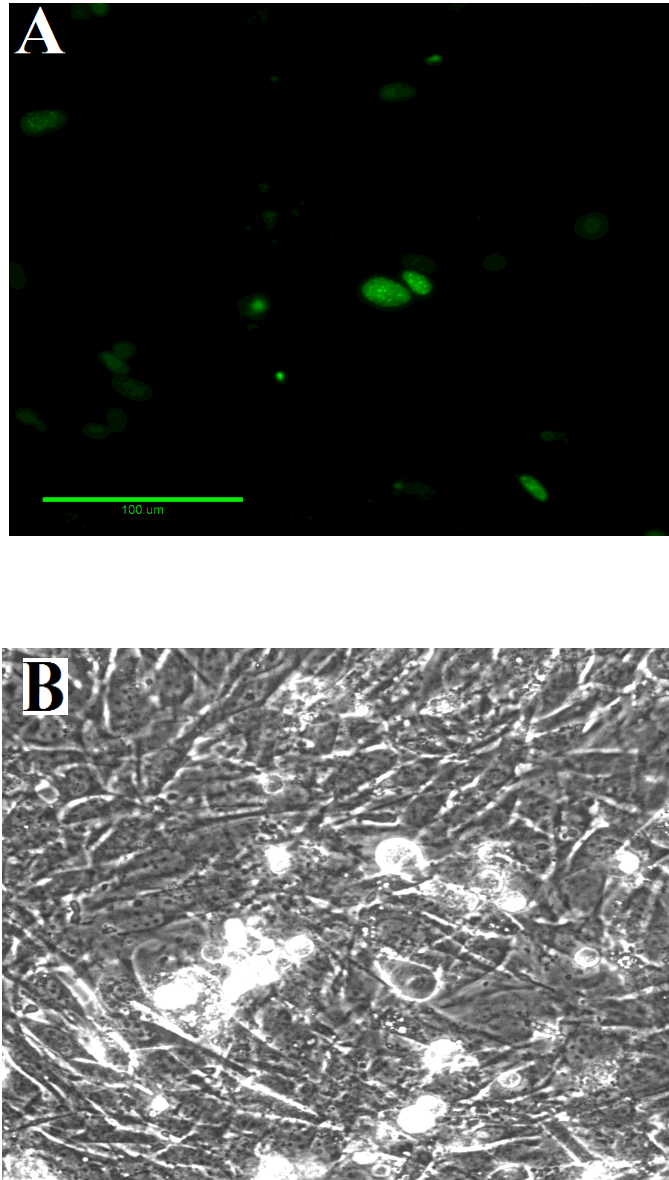


Figure 4: Transfection of HP1 $\beta$  into CGR8 cells (A) Expression of HP1 $\beta$  in MEFs (B) Phase contrast image of the MEFs transfected with HP1 $\beta$ .

### 3.3: Line-scanning Microscopy

The experiment was first attempted using unmodified CGR8 cells on the Olympus FluoView FV1000 IX2 Inverted Confocal microscope. Fluorescence readings were obtained at a resolution of 82nm/pixel with a 2 $\mu$ sec/pixel dwell time. Data was

successfully obtained which showed an oscillatory motion of the ESC DNA (Figure 5).  $G(\tau)$ , the spatial distribution of the chromatin as a function of time, is plotted as a function of time. Because we are comparing the data to itself, this is known as an autocorrelation function, enabling us to reveal repetitive data. If  $G(\tau) > 0$ , then that piece of data is said to autocorrelate; that is, the position of the chromatin is repetitively moving away and towards the same point in space at a fixed time interval. The experiments were repeated using the Nikon A1 Spectral Confocal microscope which had a higher resolution and a temperature controller. The high resolution and higher laser power caused rapid photobleaching to occur too quickly to obtain any meaningful data. Attempts to repeat the success of the first experiment using the Olympus microscope were unsuccessful due to movement of the cells, presumably caused by temperature fluctuations and subsequent pressure differentials. The experiment was halted due to the equipment difficulties.

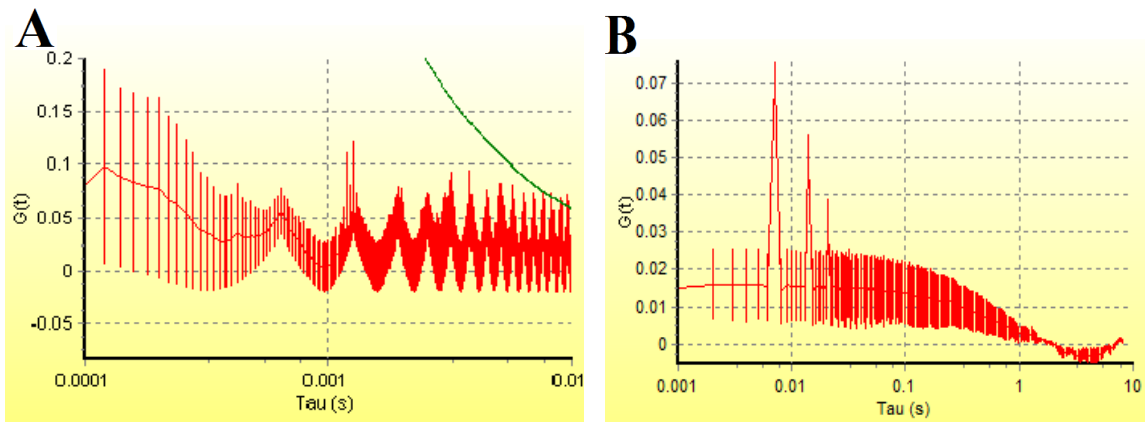


Figure 5: Vibratory motion of chromatin in ESC (A) Autocorrelation function of CGR8 chromatin. Tau (s) = time.  $G(\tau)$  = Gaussian distribution of fluorescence intensity as a function of time. Green line = Total average autocorrelation function (B) Autocorrelation function of MEF chromatin. Total average autocorrelation function not shown

### 3.4: Cloning of Ppiases

#### 3.4.1: qRT-PCR

To identify cyclophilins enriched in ESC we compared undifferentiated and differentiated TC4 and TC4 cells from previously prepared RNA-seq data. TC4 cells are undifferentiated at day one (termed TC4 d0) and are differentiated 4 days after the addition of tetracycline (TC4 d4). In addition, we compared mouse embryonic fibroblasts (MEFs) to CGR8 cells from previously prepared microarray data. Due to the inconsistency in the results, we decided to conduct a qRT-PCR of the TC4 cells and the MEF/CGR8 cells. The results of the qRT-PCR showed that PpiB and PpiC were the most heavily downregulated Ppiases upon differentiation (Figure 6). This was true in both the TC4 cells and the MEF/CGR8 comparison. All other Ppiases were upregulated in TC4 cells but were downregulated in the CGR/MEF comparison. As a result, we focused on PpiB and PpiC. In addition, we randomly chose to focus on PpiD and PpiH.

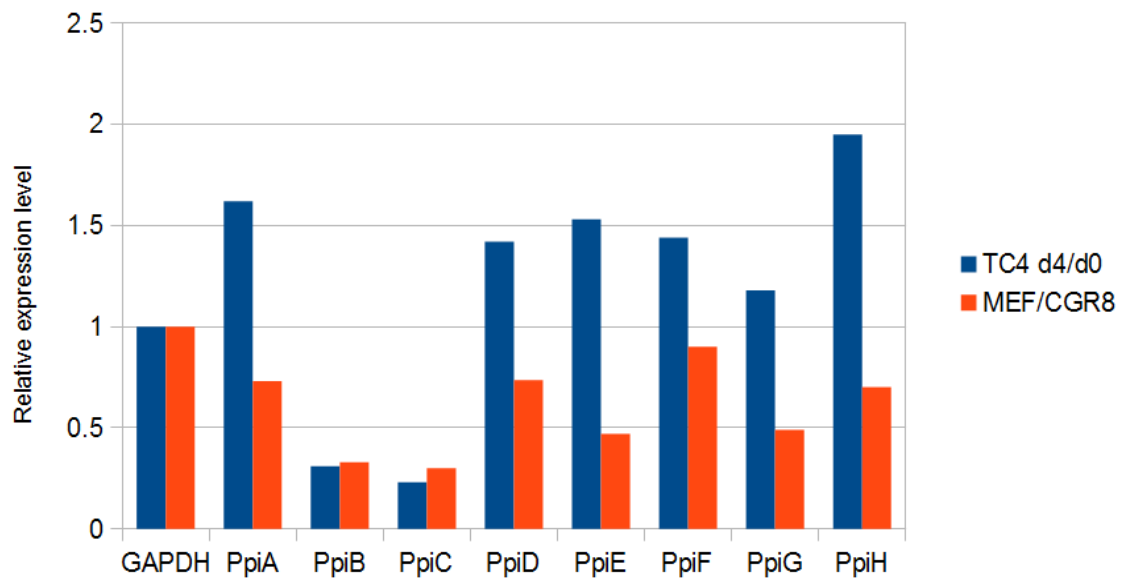


Figure 6: qRT-PCR expression ratios of MEF:CGR8 and TC4 d4:TC4 d0

### 3.4.2: Cloning of PpiB, PpiC, PpiD and PpiH into expression vectors

Cloning of PpiB from mESC cDNA was successful, producing a single band which corresponded to the correct size of PpiB (Figure 7A). The PCR of PpiC was unsuccessful, producing a band that was much too small to be PpiC. PpiH was successfully amplified, but with several extra bands. The PCR for PpiC was repeated with a higher annealing temperature. This resulted in no band produced. Several other parameters were tried but with no positive results. The PCR for PpiD was successful, producing a band of 1.1kb (Figure 7). Consequently, we shifted our focus to PpiB (due to the qRT-PCR data) and PpiD (due to its previously successful amplification).

The gene products from PpiB and PpiD were extracted and purified. The gene products were then ligated into the pET-21-c(+) plasmid. The ligation and/or transformation was unsuccessful. A higher concentration of insert was used. The ligation again failed. Several new variables were tested, including new competent cells, new ligation buffer, the addition of polynucleotide kinase (PNK) and newly autoclaved water. All of these trials were unsuccessful.

To determine where the problem in the ligation was occurring, a troubleshooting experiment was set up. pET-21-c(+) was digested with NdeI and was either gel-purified or column-purified along with a negative ligase control, for a total of three trials. No colonies were found on the gel-purified plate. 200+ colonies were found on the column-purified plate with ligase. 6 colonies were found on the column-purified plate without ligase. It was concluded that something within the gel-purification kit was interfering

with the ligation. New agarose was then used unsuccessfully. It was determined that it was another step within the gel-purification process that was going awry.

To narrow down what exactly within the gel-purification kit was causing the troubles, another troubleshooting experiment was set up. New DNA dye was used to load the DNA into the gel. New TAE buffer was used as well. In addition, newly autoclaved water was used to make new gels. None of these trials were successful.

The PCR was repeated. The gene product and plasmid were not gel-purified but were column-purified. The ligation was carried out along with a negative ligase control to determine how much closed-circle DNA was present. The ligation was successful and produced some colonies that had the correct insert. Due to the length of the insert, we decided to sequence only the first 500bp of the 5' end. The sequence of this section was a 100% match to the reported sequence.

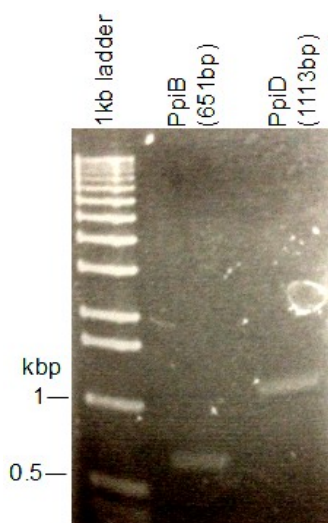


Figure 7: Amplification of PpiB and PpiD



## **4: Discussion**

### **4.1: Histone variants**

While I was able to successfully clone the testis-specific histone variant H3T, the experiment was stopped before I could begin to assess its role in the opening of chromatin nor was I able to express it along with the Yamanaka factors in MEFs in order to measure its ability to enhance reprogramming. This is because a paper came out which addressed the issue of histone variants in reprogramming [24]. This study found that overexpression of the testis-specific histone variants TH2A and TH2B did increase conventional reprogramming efficiency. They achieved frequencies up to 20-fold higher than the Yamanaka factors alone. However, these researchers did not thoroughly

investigate whether these factors induced an open chromatin conformational change. To measure chromatin dynamics, they only used DNase I and MNase sensitivity assays. While sensitivity to these assays is a hallmark of open chromatin, more data needs to be generated that support this hypothesis. In addition, they looked at different histone variants than I studied, so it is still possible that these histone variants could have increased reprogramming even further. However, this experiment was stopped due to its loss of novelty with the release of the study on TH2A and TH2B [24].

## 4.2 Ppiase cloning

The cloning of PpiB was a success, but experiments did not advance far enough for me to assess its ability to influence chromatin dynamics. Future experiments will use this pET21-c(+)-PpiB construct to express PpiB in bacteria, purify the PpiB protein and perform a Ppiase assay (see section 1.5) to determine if it is able to isomerize any of the histone tails. Additionally, future experiments might investigate whether the Ppiases have isomerase activity for a specific protein *in vivo*. One method that has been used to demonstrate Pin1 isomerase activity *in vivo* is to isolate and crystallize proteins that interact with Pin1 and use NMR spectroscopy to identify *cis* versus *trans* conformations [50]. Another method of investigating *in vivo* isomerase activity is by inserting point mutations into the genome which would generate mutants proteins that would be unable to interact with the Ppiase. This method was used by one group of researchers to show that Pin1-dependent CtIP isomerization was abated when the mutations were present [49]. In addition, another previous study identified proteins that Pin1 interacted with by

using a glutathione S-transferase-Pin1 fusion protein [48] and then used *in vitro* screening methods to determine which proteins Pin1 could potentially isomerize *in vivo*. Similar methods could be used to demonstrate isomerase activity for our Ppiases.

Following these experiments, PpiB and the other Ppiases will be assessed for their ability to induce hyperdynamic chromatin and to enhance reprogramming using OSKM.

### **4.3 Heterochromatin binding proteins**

HP1 $\alpha$ , HP1 $\beta$  and Ezh2 were all successfully cloned into a mammalian expression vector containing conjugated GFP. Transfection of HP1 $\alpha$  and HP1 $\beta$  into MEFs was successful, at an efficiency of 5% and 1-2%, respectively. Although this experiment was stopped, future experiments will use these constructs as a tool to determine the accessibility of chromatin via FRAP. FRAP will then be used as a tool to measure the ability of other factors to influence chromatin dynamics.

### **4.4 Line-scanning microscopy**

Line-scanning microscopy is a very promising tool for visualizing molecular structures, but technically challenging. The autocorrelation function, a valuable mathematical tool, is a measure of the similarity of the position of chromatin in terms of the time period between the two similar data points. Put simply, if the DNA repeatedly moves away from the center and then returns, the autocorrelation function will oscillate as well, as shown in Figure 5. While this data is promising, no other data set from the CGR8 cells showed such a distinct oscillation. Additionally, this data was achieved at a

lower resolution than would be required for proper analysis. This experiment was done at a resolution of 82nm/pixel and 32 pixels per line scan, meaning that each line scan covered 2.6µm. If this data is to be believed, the amplitude of vibrations must be greater than 82nm, which is higher than the size of condensed histones (approximately 32nm, see introduction). Most importantly, this was not done in a temperature controlled environment. Heat could have caused the vibrational movement seen. This experiment should be repeated at a higher resolution and with temperature controlled environment.

## 5: Bibliography

- [1] Takahashi K., et al. Induction of pluripotent stem cells from mouse embryonic and adult fibroblast cultures by defined factors. *Cell*. 2006 Aug 25;126(4):663-76. Epub 2006 Aug 10.
- [2] Ruetz T., et al. Routes to induced pluripotent stem cells. *Curr Opin Genet Dev*. 2014 Sep 2;28C:38-42. [Epub ahead of print]
- [3] Briggs R., et al. Transplantation of Living Nuclei From Blastula Cells into Enucleated Frogs' Eggs. *Proc Natl Acad Sci U S A*. 1952 May;38(5):455-63.
- [4] Gurdon J., The developmental capacity of nuclei taken from intestinal epithelium cells of feeding tadpoles. *J Embryol Exp Morphol*. 1962 Dec;10:622-40.
- [5] Liu K., et al. Understanding the roadmaps to induced pluripotency. *Cell Death Dis*. 2014 May 15;5:e1232.
- [6] Tada M., et al. Nuclear reprogramming of somatic cells by in vitro hybridization with ES cells. *Curr Biol*. 2001 Oct 2;11(19):1553-8.
- [7] Yu J., et al. Induced pluripotent stem cell lines derived from human somatic cells. *Science*. 2007 Dec 21;318(5858):1917-20. Epub 2007 Nov 20.
- [8] Okita K., et al. Generation of mouse induced pluripotent stem cells without viral vectors. *Science*. 2008 Nov 7;322(5903):949-53. Epub 2008 Oct 9.
- [9] Hou P., et al. Pluripotent stem cells induced from mouse somatic cells by small-

- molecule compounds. *Science*. 2013 Aug 9;341(6146):651-4. Epub 2013 Jul 18.
- [10] Sohn YD., et al. Generation of induced pluripotent stem cells from somatic cells. *Prog Mol Biol Transl Sci*. 2012;111:1-26.
- [11] Cho H.J., et al. Induction of pluripotent stem cells from adult somatic cells by protein-based reprogramming without genetic manipulation. *Blood*, 116 (2010), pp. 386–395
- [12] Anokye-Danso F., et al. Highly efficient miRNA-mediated reprogramming of mouse and human somatic cells to pluripotency. *Cell Stem Cell*, 8 (2011), pp. 376–388
- [13] Ramalho-Santos M., et al. iPS cells: insights into basic biology. *Cell*, 138 (2009), pp. 616–618
- [14] Kobayashi H., et al. Epigenetic regulation of open chromatin in pluripotent stem cells. *Transl Res*. 2014 Mar 13. [Epub ahead of print]
- [15] Dessypris E., et al. Erythropoiesis. *Wintrobe's clinical hematology (12th ed.)*, (2009), pp. 106–125
- [16] Skubitz K., et al. Neutrophilic leukocytes. *Wintrobe's clinical hematology (12th ed.)*, (2009), pp. 170–213
- [17] Eckfeldt C.E., et al. The molecular repertoire of the “almighty” stem cell. *Nat Rev Mol Cell Biol*, 6 (2005), pp. 726–737
- [18] Efroni S., et al. Global transcription in pluripotent embryonic stem cells. *Cell Stem Cell*, 2 (2008), pp. 437–447
- [19] Koche RP, et al. Reprogramming factor expression initiates widespread targeted chromatin remodeling. *Cell Stem Cell*. 2011 Jan 7;8(1):96-105.
- [20] Gaspar-Maia A., et al. Open chromatin in pluripotency and reprogramming. *Nat Rev Mol Cell Biol*, 12 (2011), pp. 36–47
- [21] Meshorer E., et al. Hyperdynamic plasticity of chromatin proteins in pluripotent embryonic stem cells. *Dev Cell*. 2006 Jan;10(1):105-16.
- [22] Clapier C.R., et al. The biology of chromatin remodeling complexes. *Annu Rev Biochem*, 78 (2009), pp. 273–304
- [23] Banaszynski L.A., et al. Histone variants in metazoan development. *Dev Cell*. 2010 Nov 16;19(5):662-74.
- [24] Shinagawa T., et al. Histone variants enriched in oocytes enhance reprogramming to induced pluripotent stem cells. *Cell Stem Cell*. 2014 Feb 6;14(2):217-27
- [25] Witt O., et al. Testis-specific expression of a novel human H3 histone gene. *Exp Cell Res*. 1996 Dec 15;229(2):301-6.
- [26] Bernstein B.E., et al. A bivalent chromatin structure marks key developmental genes in embryonic stem cells. *Cell*. 2006 Apr 21;125(2):315-26.
- [27] Brumbaugh J., et al. Removing reprogramming roadblocks: Mbd3 depletion allows deterministic iPSC generation. *Cell Stem Cell*. 2013 Oct 3;13(4):379-81.
- [28] Luo M., et al. NuRD blocks reprogramming of mouse somatic cells into pluripotent stem cells. *Stem Cells*. 2013 Jul;31(7):1278-86.
- [29] Kalkan T., et al. Mapping the route from naive pluripotency to lineage specification. *Philos Trans R Soc Lond B Biol Sci*. 2014 Dec 5;369(1657).
- [30] Gaspar-Maia A., et al. Chd1 regulates open chromatin and pluripotency of embryonic stem cells. *Nature*. 2009 Aug 13;460(7257):863-8. Epub 2009 Jul 8.

- [31] Skene P.J., et al. Histone variants in pluripotency and disease. *Development*. 2013 Jun;140(12):2513-24.
- [32] Hu G., et al. H2A.Z facilitates access of active and repressive complexes to chromatin in embryonic stem cell self-renewal and differentiation. *Cell Stem Cell*. 2013 Feb 7;12(2):180-92. Epub 2012 Dec 20.
- [33] Goldberg A., et al. Distinct factors control histone variant H3.3 localization at specific genomic regions. *Cell* (2010) 140, 678-691
- [34] Soboleva T.A., et al. A unique H2A histone variant occupies the transcriptional start site of active genes. *Nat Struct Mol Biol*. 2011 Dec 4;19(1):25-30.
- [35] De Carvalho D.D., et al. DNA methylation and cellular reprogramming. *Trends Cell Biol*. 2010 Oct;20(10):609-17. Epub 2010 Aug 31.
- [36] Jullien J., et al. HIRA dependent H3.3 deposition is required for transcriptional reprogramming following nuclear transfer to *Xenopus* oocytes. *Epigenetics Chromatin*. 2012 Oct 29;5(1):17.
- [37] Tachiwana H., et al. Structural basis of instability of the nucleosome containing a testis-specific histone variant, humanH3T. *Proc Natl Acad Sci U S A*. 2010 Jun 8;107(23):10454-9. Epub 2010 May 24.
- [38] Hammoud S.S., et al. Distinctive chromatin in human sperm packages genes for embryo development. *Nature*. 2009 Jul 23; 460(7254):473-8.
- [39] Arimura Y., et al. Structural basis of a nucleosome containing histone H2A.B/H2A.Bbd that transiently associates with reorganized chromatin. *Sci Rep*. 2013 Dec 16;3:3510.
- [40] Hinde E., et al. Tracking the mechanical dynamics of human embryonic stem cell chromatin. *Epigenetics Chromatin*. 2012 Dec 21;5(1):20.
- [41] Gollan P.J., et al. The FKBP families of higher plants: Exploring the structures and functions of protein interaction specialists. *FEBS Lett*. 2012 Oct 19;586(20):3539-47. Epub 2012 Sep 13.
- [42] Farrell A.S., et al. Pin1 regulates the dynamics of c-Myc DNA binding to facilitate target gene regulation and oncogenesis. *Mol Cell Biol*. 2013 Aug;33(15):2930-49. Epub 2013 May 28.
- [43] Monneau Y.R., et al. Structure and activity of the peptidyl-prolyl isomerase domain from the histone chaperone Fpr4 toward histone H3 proline isomerization. *J Biol Chem*. 2013 Sep 6;288(36):25826-37. Epub 2013 Jul 25.
- [44] Elrod J.W., et al. Physiologic functions of cyclophilin D and the mitochondrial permeability transition pore. *Circ J*. 2013;77(5):1111-22. Epub 2013 Mar 29.
- [45] Doshi U., et al. The dilemma of conformational dynamics in enzyme catalysis: perspectives from theory and experiment. *Adv Exp Med Biol*. 2014;805:221-43.
- [46] Kofron J.L., et al. Determination of kinetic constants for peptidyl prolyl cis-trans isomerases by an improved spectrophotometric assay. *Biochemistry*. 1991 Jun 25;30(25):6127-34.
- [47] Příkrylová T., et al. Epigenetics and chromatin plasticity in embryonic stem cells. *World J Stem Cells*. Jul 26, 2013; 5(3): 73-85
- [48] Yaffe M.B., Sequence-specific and phosphorylation-dependent proline isomerization: a potential mitotic regulatory mechanism. *Science*. 1997 Dec

12;278(5345):1957-60.

[49] Steger M., Prolyl isomerase PIN1 regulates DNA double-strand break repair by counteracting DNA end resection. *Mol Cell*. 2013 May 9;50(3):333-43.

[50] Lippens G., Molecular mechanisms of the phospho-dependent prolyl cis/trans isomerase Pin1. *FEBS J*. 2007 Oct;274(20):5211-22. Epub 2007 Sep 24.